

γ strength functions in ^{60}Ni from two-step cascades following proton capture

A. Voinov,^{1,*} S.M. Grimes,¹ C.R. Brune,¹ M. Guttormsen,² A.C. Larsen,² T.N. Massey,¹ A. Schiller,¹ and S. Siem²

¹*Department of Physics and Astronomy, Ohio University, Athens, OH 45701, USA*

²*Department of Physics, University of Oslo, N-0316 Oslo, Norway*

The two-step cascade method previously used in neutron capture experiments is now applied to a proton capture reaction. The spectrum of two-step cascades populating the first 2^+ level of ^{60}Ni has been measured with $^{59}\text{Co}(p, 2\gamma)^{60}\text{Ni}$ reaction. The simulation technique used for the spectrum analysis allows one to reveal the range of possible shapes of both $E1$ and $M1$ γ -strength functions. The low-energy enhancement previously observed in ^3He induced reactions is seen to appear in $M1$ strength functions of ^{60}Ni .

PACS numbers: 25.40.Lw, 25.20.Lj, 27.50.+e

I. INTRODUCTION

The $E1$ and $M1$ γ -strength functions below the particle separation threshold are still a subject of investigation and a source of large uncertainties in reaction cross-section calculations [1]. Despite the long history of experimental studies, no definite results have been established for this energy region. The current status of γ -strength functions is summarized in Ref. [2], where the $E1$ strength is described on the basis of a low-energy extrapolation of the giant dipole resonance (GDR). Usually a modified Lorentz function is applied, taking into account the energy and temperature dependence of the GDR width. The $M1$ strength is described by the Lorentz function based on the existence of the spin-flip $M1$ resonance. However, the parameters of this resonance (peak cross-section, width, and centroid) suffer from large uncertainties.

Experimental information about γ -strength functions for γ -transitions below the particle separation energy can be obtained from measuring the γ -spectra of different nuclear reactions. However, since the spectra depend not only on the γ -strength functions but also on the density of levels populated by the γ -transitions, the interpretation of such spectra is difficult. All γ -strength function models recommended in Ref. [2] are in fact dependent on the level density model applied, since they were basically obtained from γ -spectra of neutron capture reactions. Thus, it was necessary to assume a model for the level density below the neutron binding energy in order to derive a model for the γ -strength.

At present, there is an increasing interest in nuclear γ -strength functions. For example, the recent finding of an $E1$ pygmy dipole resonance below the neutron threshold for ^{136}Xe from $(\gamma\gamma')$ experiments [3] and for ^{117}Sn [4] from $(^3\text{He}, ^3\text{He}')$ experiments is very intriguing and could have a large impact on reaction rates relevant for nuclear astrophysics. Also, new experimental techniques which allows one to study γ -strength functions below the neu-

tron separation energy with photon absorption reactions are developed [5].

An unexpected enhancement of the low-energy part of the γ -strength function has been reported for nuclei from the medium-mass region such as $^{56,57}\text{Fe}$ [6, 7] and $^{50,51}\text{V}$ [8], and for the heavier $^{93-98}\text{Mo}$ [9]. These results are obtained with ^3He -induced reactions where the particle- γ coincidence data has been analyzed with the so-called Oslo method (Oslo-type experiments). The question of whether this behavior is unique to these nuclei or if it is a general feature of a certain mass region is open and requires further investigations.

At this point it is clear that there is no single experiment which would give a complete picture of the γ -strength functions in a wide energy range. Different experimental techniques need to be combined to gradually uncover the various structures and the underlying physics of the γ -strength function.

One of the experimental techniques successfully applied to test γ -strength function models is the method of two-step γ -cascades (TSC) following thermal neutron capture. It was first proposed by Hoogenboom [10] and later developed by the Dubna group [11] and the Prague group [12]. The idea of this method is to obtain spectra of cascade γ -transitions proceeding between compound levels and one of the low-lying discrete levels of the final nucleus. The sum energy of such two-step cascades is fixed and the shape of the TSC spectra is determined by the level density and the γ -strength function of the final nucleus. This method has proven to be a relatively sensitive test. However, it might suffer from large uncertainties mainly due to unknown level density functions (one must usually rely on models) and large Porter-Thomas (PT) fluctuations of the cascade intensities. Therefore, the description of the shape of the TSC spectra can be rather uncertain. For the absolute normalization of the TSC intensities one uses literature data on absolute intensities of primary γ -transitions and branching ratios of low-lying levels. Both these quantities, especially the latter, are usually not known with high enough precision.

In order to reduce the uncertainties related to the TSC method for neutron capture reactions, we measured the TSC spectrum from the proton capture reac-

*Electronic address: voinov@ohio.edu

tion $^{59}\text{Co}(p, 2\gamma)^{60}\text{Ni}$. In this work, the novel approach is that the level density of the final nucleus ^{60}Ni has been obtained by us in an independent experiment utilizing neutron evaporation spectra. This simplified the analysis of the TSC spectrum considerably. Also, the great advantage of proton capture is that due to the proton energy spread in the target, many compound nuclear resonances are excited. Thus, a good averaging of the resonance decay properties is provided and the PT fluctuations are reduced.

In this article we describe our first results on TSC γ -transitions populating the first 2^+ level of the final ^{60}Ni nucleus from the proton capture on ^{59}Co .

II. EXPERIMENT AND METHOD

Cascade γ -transitions following the proton capture on ^{59}Co have been measured with two high-purity germanium (HPGe) detectors (40% and 60% efficiency) placed at about 8 cm from the target, making an angle of about 125° to reduce possible anisotropy effects of the cascades caused by angular correlations. Lead discs of 1-mm thickness were placed in front of each detector in order to reduce cross-talk effects. The tandem accelerator of Edwards Accelerator Laboratory, Ohio University, delivered the proton beam with energy of 1.85 MeV, which is just below the (p, n) reaction threshold. At this energy, along with the (p, γ) channel, only the (p, α) channel is open. The latter channel does not produce significant γ emission because of its small cross section. A 1- μm thick natural cobalt foil (100% ^{59}Co) was used as target. The energy loss in the target was estimated to be around 80 keV. The beam current was maintained at about 150-200 nA to keep the counting rate of each detector at about 3000/sec. Single spectra and coincident events were accumulated simultaneously. Considering the energy spread due to the energy loss in the target, the number of proton-capture resonances excited are estimated to be ~ 70 . Therefore, a good averaging is provided, which ensures a sufficient independence of the decay properties of the individual resonances.

The spectrum of the sum amplitude of two coincident pulses is shown in Fig. 1. Two-step γ -cascades create peaks in such a spectrum revealing the population of discrete low-lying levels. One can see a very small peak at 11.3 MeV corresponding to the population of the ground state of ^{60}Ni , the large peak populating the first 2^+ excited state as well as satellite peaks caused by single-escape annihilation quanta. These peaks have a width of around 80 keV, which is consistent with the proton energy loss in the target. This width is considerably larger than for similar experiments with thermal neutrons, where the peak widths are limited by the detector resolution only. The Compton background increases considerably as the energy decreases. Thus, only the 2^+ peak has a reasonable peak-to-background ratio in this experiment. This peak was therefore used to create the

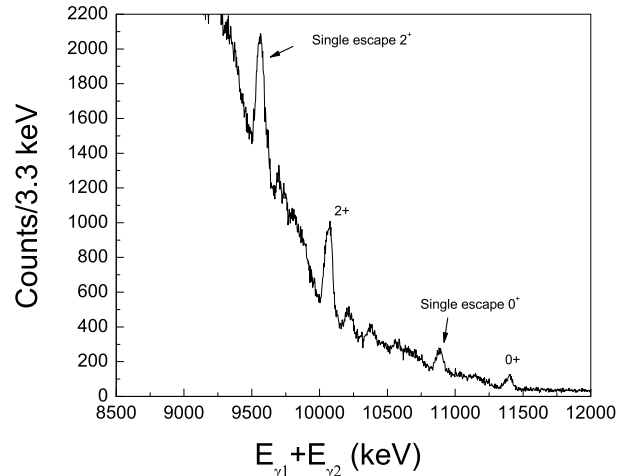


FIG. 1: The spectrum of the sum amplitude of two coincident pulses from the $^{59}\text{Co}(p, 2\gamma)^{60}\text{Ni}$ reaction.

corresponding TSC spectrum. This spectrum is made by placing a gate on the peak and subtracting the spectra obtained by gating on the background at both sides of the peak (for details, see [12]). The resulting cascade spectrum corrected for the detector efficiencies is shown in Fig. 2. This spectrum consists of the full-energy absorption peaks only, which are well separated in the low-energy range and become a smooth distribution towards the center of the spectrum. The low-energy part of the spectrum is free from any cross-talk effects including low-energy bremsstrahlung as discussed in Ref. [13].

The efficiency of the detectors has been determined by measuring the γ -spectrum from the $^{27}\text{Al}(p, \gamma)$ reaction at $E_p = 0.992$ MeV and using the standard γ -intensities for this reaction from Ref. [14].

Ideally, the TSC spectrum should be symmetric in respect to half of the sum energy of two cascades $(E_{\gamma_1} + E_{\gamma_2})/2$ because each cascade creates full absorption peaks at two places in the spectrum, at E_{γ_1} and at E_{γ_2} . However, due to different energy resolutions, the high-energy discrete peaks are considerably broader compared to their low-energy satellites.

We also accumulated the singles γ -ray spectrum with energies from 0.3 to 12 MeV. The primary interest here is the $2^+ \rightarrow 0^+$ 1332-keV γ transition since its absolute intensity consists of more than 90% of the compound ^{60}Ni nucleus decays. The intensity of cascade transitions was determined relative to the intensity of this 1332 keV γ -transition. In the following, this normalized TSC spectrum is analyzed to obtain the γ -ray strength function.

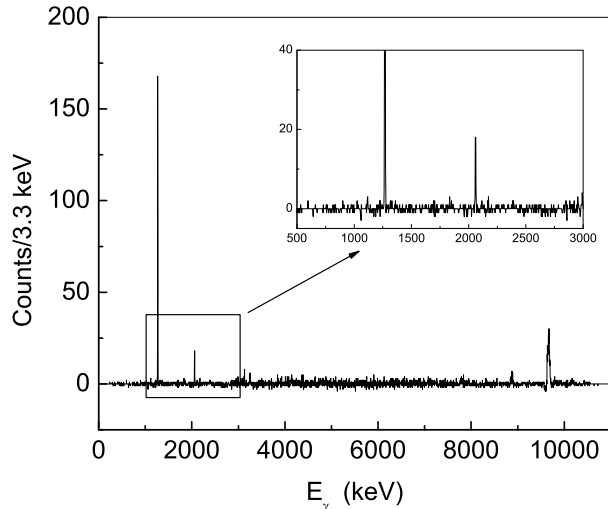


FIG. 2: The spectrum of two-step γ -transitions populating the 2^+ level of the ^{60}Ni nucleus.

III. COMPARISON WITH MODEL CALCULATIONS

In order to reduce the PT fluctuations of the individual cascades, the TSC spectrum in Fig. 2 was compressed into 500-keV energy bins. Assuming that the proton capture at this energy is due to the compound reaction mechanism, the shape and the absolute intensity of the spectrum is determined by the $E1$, $M1$, and (to a lesser extent) the $E2$ strength functions of both the primary and the secondary γ -transitions in the cascades. It is also determined by the level density of the residual nucleus ^{60}Ni .

A. Level density and γ -strength functions

Traditionally, the level density was one of the most uncertain quantities when analyzing γ -spectra from nuclear reactions. In our case the level density has been obtained by us from the reactions $^{59}\text{Co}(d, n)^{60}\text{Ni}$, $^{58}\text{Fe}(^3\text{He}, n)^{60}\text{Ni}$ [6] and $^{55}\text{Mn}(^6\text{Li}, n)^{60}\text{Ni}$ [15]. Based on these experiments, it turned out that it is more appropriate to use the constant-temperature level density $\rho(U) = 1/T \exp((E - E_0)/T)$ (compared to the Fermi-gas model with $T \sim \sqrt{E}$) with a temperature of $T = 1.4$ MeV and an energy shift of $E_0 = -0.85$ MeV.

Another important feature affecting the calculations is the ratio of levels with positive and negative parities. Usually, the number of positive and negative levels are assumed to be equal in level-density model calculations. However, this is not the case for the ^{60}Ni where, as seen from the level scheme, the deviation from the parity balance is obvious and can no longer be neglected. Up to

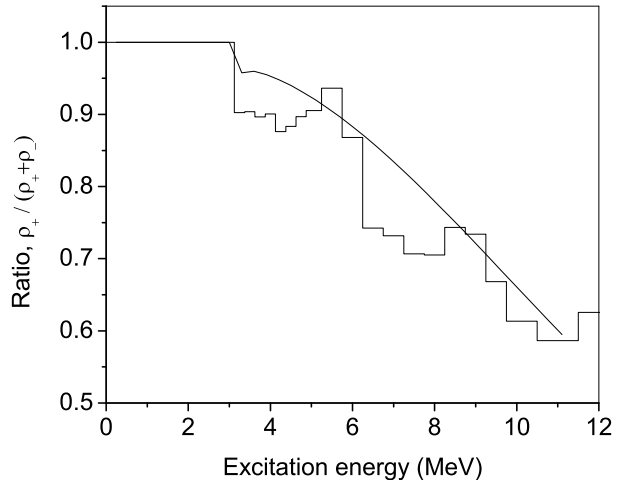


FIG. 3: Ratio of the density of positive parity levels to the total level density for ^{60}Ni . The histogram represents the calculations of Ref. [16]. The line shows the approximation used in our calculations.

4.2 MeV of excitation energy, ^{60}Ni has only one level of negative parity, while the rest have positive parity. The parity ratio above 4.2 MeV must be estimated on the basis of model calculations. We have used the calculations of Ref. [16] based on the HF-BCS microscopical approach. The result of these calculations for ^{60}Ni and the approximation we have applied in our TSC calculations are presented in Fig. 3.

We have tested the most commonly used prescriptions for the γ -strength functions. The first and most traditional one is the standard Lorentzian (SLO) function for $E1$ transitions with parameters fitted to the GDR [2]. There are also models which take into account the temperature dependence of the γ -strength such as the Kadmsky-Markushev-Furman (KMF) model [17] and the generalized Lorentzian (GLO) [18]. The $M1$ and $E2$ γ -strength functions are more uncertain. For both of them we used the standard Lorentzian function with parameters based on the recommended systematics of Ref. [2]. For the $M1$ strength, the single-particle (SP) energy independent function [19] has been tested as well.

The spin distribution of the compound levels populated through 1.85-MeV proton capture can be estimated on the basis of a proton optical potential which determines the transmission coefficients for each orbital momentum of the captured proton. There are three different potentials available in the RIPL data base [2]. For these three potentials, we estimated the following fractions of the capture cross section for the different ℓ values of the captured protons: 0.64, 0.55 and 0.52 for s-wave protons; 0.15, 0.27 and 0.30 for p-wave protons; and 0.20, 0.17, and 0.17 for d-wave protons. We tested all three potentials in our simulations and found that, within the uncertainties, our final results did not depend on the particular

TABLE I: Ratio of calculated and experimental intensities for cascades populating the 2^+ level of ^{60}Ni .

$E1+M1$ models	Energy interval, MeV		
	0.5-2	2.15-3.4	4-5.1
KMF+SLO	0.87(17)	3.10(120)	1.84(37)
KMF+SP	0.58(12)	1.74(70)	1.08(21)
SLO+SLO	0.64(13)	2.45(100)	1.58(32)
SLO+SP	0.48(10)	1.56(60)	1.10(22)
GLO+SLO	0.51(10)	1.81(72)	1.24(25)
GLO+SP	0.38(8)	1.11(44)	0.71(14)

potential used. The results we present here is based on the optical potential of Ref. [20] (corresponding to the first numbers of the given fractions above).

In order to compare the experimental TSC spectrum with the calculations we have chosen three energy intervals of the spectrum of Fig. 2. These intervals reflect the most important features of the spectrum and determine the spectral shape. One can see from Table I that the main problem of all the models is that they are not able to simultaneously describe the first and the second energy interval of the spectrum, although many models describe well the cascade intensity in the third energy interval belonging to the middle part of the spectrum. This result shows that analyzing just the middle part of the spectrum is not sufficient to unambiguously test γ -strength functions with TSC spectra. Here we can use the advantage of the $(p, 2\gamma)$ reaction compared to the $(n, 2\gamma)$ reaction: in the case of neutron capture reactions only the middle part of the TSC spectra is usually compared with calculations due to increasing PT fluctuations in other energy intervals [12].

B. Simulations

In order to find the range of possible $E1$ and $M1$ γ -strength function shapes which would describe the TSC spectrum, we simulated the TSC spectrum with randomly shaped input strength functions. The range of input strength function shapes has been determined taking into account the current knowledge about the possible forms of their energy dependence. Since most models are based on the Lorentz function, we have chosen this as a basic function to describe both $E1$ and $M1$ γ -strength below the particle threshold. In addition to that, an exponential low-energy enhancement function has been added to mimic the possible alteration of the Lorentz function in the low-energy intervals. The possible uncertainties in the general slope have been simulated using the multiplication term of the form $\exp[A(E_\gamma - 11.3)]$, where the number 11.3 is chosen to be equal to the excitation energy (in MeV) of the compound nucleus and A is the coefficient determining the slope. This gives the functional form of both $E1$ and $M1$ strength functions

as:

$$f = 8.68 \cdot 10^{-8} (\text{mb}^{-1} \text{ MeV}^{-2}) \times C_{M1} \left[\frac{E_\gamma \Gamma}{(E_\gamma^2 - E_r^2)^2 + E_\gamma^2 \Gamma} + B \exp(-CE_\gamma) \right] \times \exp[A(E_\gamma - 11.3)] \quad (1)$$

The parameters A , B , and C were varied randomly to accommodate a wide range of function shapes. The parameter C_{M1} (applied to the $M1$ strength function) varied randomly between 0.1 and 0.7 to be consistent with the experimental systematics and the corresponding uncertainties of the f_{M1}/f_{E1} ratio [2]. The parameters for the GDR has been taken from Ref. [2]. It has been tested that the function given by Eq. (1) is able to mimic all known functions currently used to model γ -strength functions, including those used previously in this paper (see Table I). The only restriction is that it assumes that the Axel-Brink hypothesis is valid, which means that the strength functions do not depend on the excitation energy of the final levels populated by the γ -transitions. This is not the case for the KMF and GLO models in which the strength depends on the temperature, which in turn depends on the intrinsic excitation energy U as the Fermi-gas model predicts ($T = \sqrt{U/a}$, where a is the level-density parameter). The temperature behavior in nuclei is an open problem and there is no conclusive experimental data in the energy range of our interest. For example, uncertainties regarding the Fermi-gas versus the constant-temperature level density models still exist. In the case of ^{60}Ni , we have showed in a previous work that the constant-temperature model works better for excitation energies up to 20 MeV [15]. Therefore we deem that the Axel-Brink hypothesis is justified for this specific nucleus in the energy region of interest.

We have simulated $E1$ and $M1$ strength functions according to Eq. (1). The $E2$ strength function has been calculated using a Lorentz function with parameters according to the systematics of Ref. [2]. For each combination of random $E1$ and $M1$ strength functions the TSC spectrum is generated. Only those spectra that agree with the experimental one within predefined uncertainties are selected. The uncertainties have been estimated to be 20, 40 and 20 percent for the first, second, and third energy intervals, respectively (see Table I).

First, to investigate how well the simulation procedure works, we used a test spectrum calculated with a set of selected input strength function models to check that the input and output strength functions are consistent. The models we chose to use were the GLO model with a constant temperature for the $E1$ strength, and the SLO model for the $M1$ strength function. Then, we simulated this spectrum with random strength functions using Eq. (1). The output strength functions that reproduce the test spectrum within the predefined uncertainties were selected. These strengths are compared with the input strength functions in Fig. 4. The absolute normalization of the strength functions does not affect the

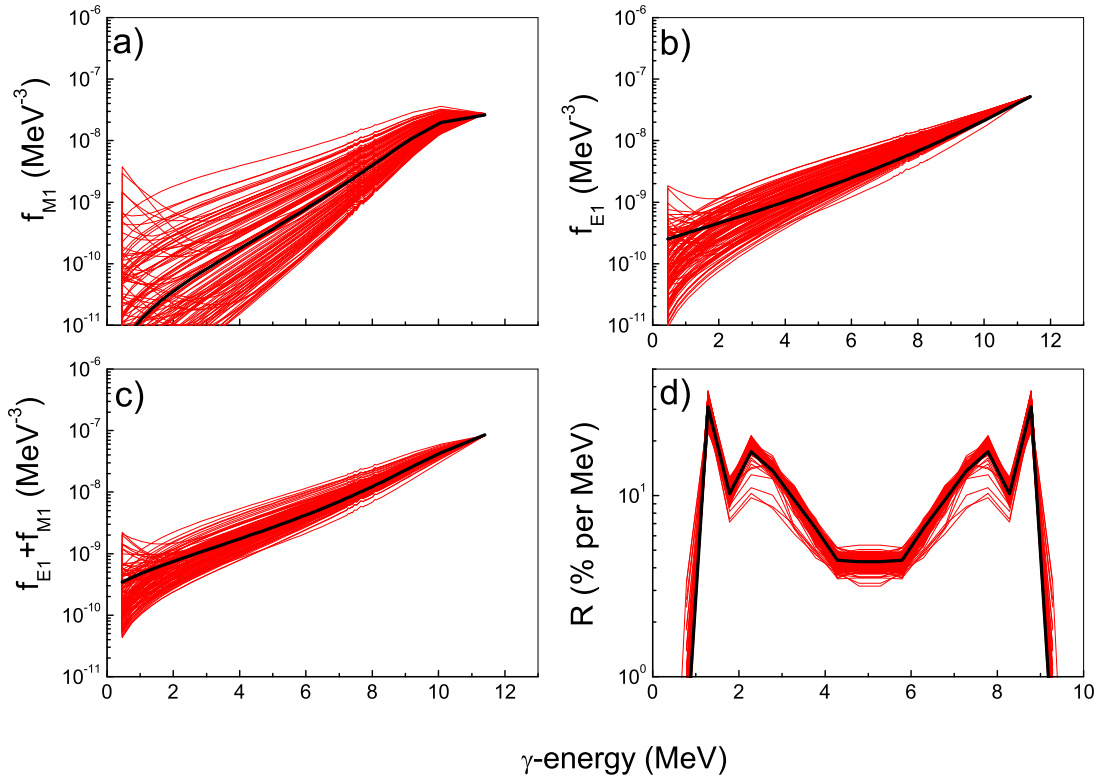


FIG. 4: (Color online) Results of the simulations of the two-step cascade spectrum populating the 2^+ level of ^{60}Ni . The black thick lines in the panels a), b), and c) are input strength functions which result in the black TSC spectrum in panel d). The thin red lines show the output functions and the corresponding TSC spectra resulting from the simulation procedure. In panel d), R is the ratio of the TSC intensity and the intensity of the $2^+ \rightarrow 0^+$ ground state transition in ^{60}Ni . Note that the absolute scale of the strength functions is approximate.

TSC calculations, only the slope is important. Therefore, in order to reveal the shape variation, all strength functions have been normalized to the same number at $E_\gamma \approx 11.3$ MeV, which is approximately consistent with the absolute scale at these γ -energies. One can see the degree of sensitivity of the cascade spectrum to the functional dependence of the strength functions. Within the adopted uncertainties of the TSC spectrum, the slopes of both the $E1$ and $M1$ strength functions exhibit large variations. However, the important result from this simulation test is that the original input strength functions are in the uncertainty corridor of the output functions. The spectrum does not appear to be sensitive to the γ -strength functions for γ -ray energies below 2 MeV. However, one should mention that in general, the degree of sensitivity can vary for different nuclei.

Next, we performed a simulation in the same way as previously described, but now we selected only those output strength functions which reproduce the experimental TSC spectrum within our predefined uncertainties in the three energy intervals. The result is shown in

Fig. 5. Although there are large uncertainties in the obtained functions, it is obvious that all the possible $M1$ strength functions show a low-energy increase. However, the $E1$ function below ~ 2 MeV is rather uncertain; this strength might have an increase at low energies, but it is equally probable to have a decreasing $E1$ strength. The sum of $E1$ and $M1$ functions exhibits less uncertainties and therefore the low-energy increase is more pronounced here. This shape is consistent with what we have observed previously in Oslo-type experiments for nuclei in this mass region, ^{56}Fe and ^{57}Fe [6, 7]. However, from the current simulation we can specify that the low-energy enhancement is most likely due to $M1$ γ -transitions.

IV. DISCUSSION

The performed simulations show that the proton-capture TSC spectra can be equally well described with a variety of $E1$ and $M1$ strength functions. However, some general trends of the γ -strength functions can be

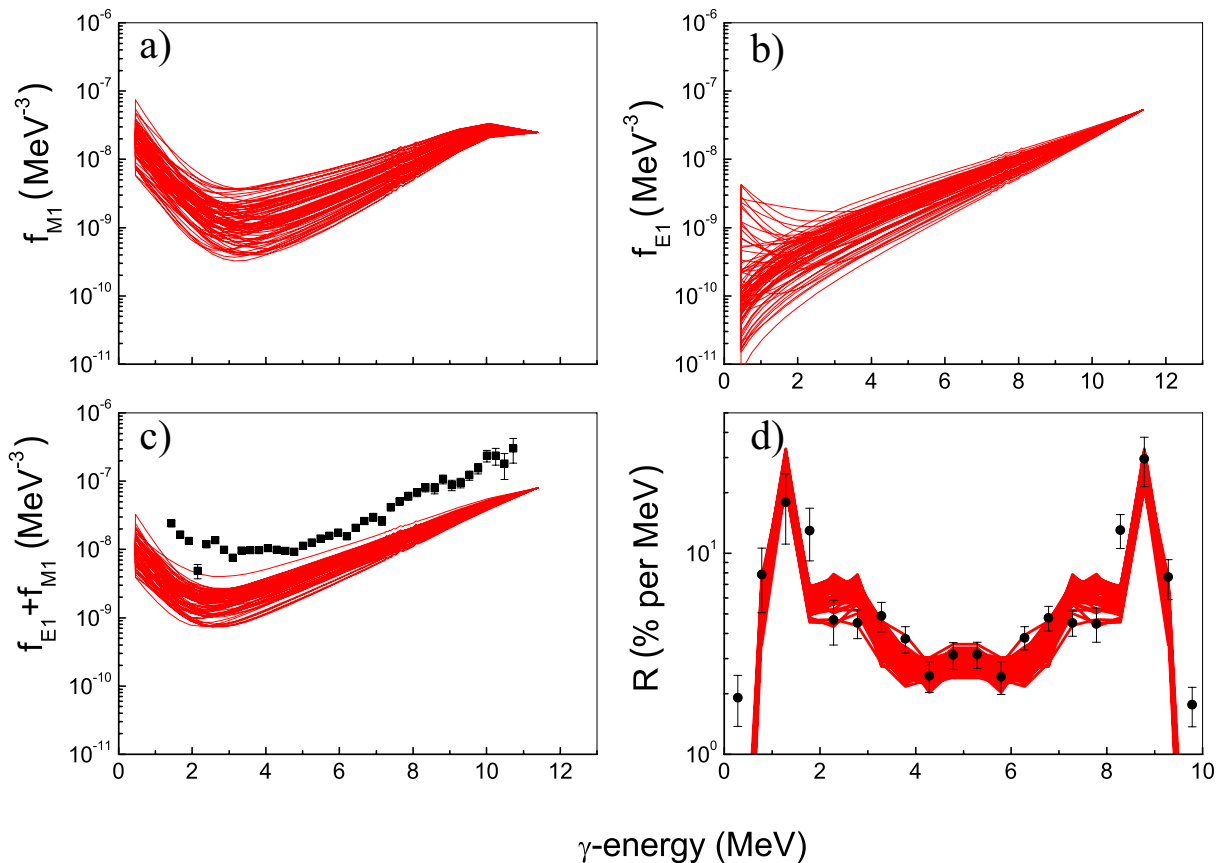


FIG. 5: Same as in Fig. 4 but for the experimental TSC spectrum. The black points in panel c) are data on ^{56}Fe from the Oslo experiment [7].

studied unambiguously with this technique.

Because there are many resonances excited in a proton capture experiment, the obtained TSC spectra are less vulnerable to PT fluctuations compared to similar spectra from thermal neutron-capture experiments. This fact considerably reduces the uncertainties of the resulting γ -strength functions. Indeed, we have performed additional simulations where only the third energy interval corresponding to the middle of the TSC spectrum was used to select output strength functions. The middle interval is traditionally used to compare experimental and theoretical TSC spectra obtained from thermal neutron capture experiments [12], since in this part of the spectrum, the number of intermediate levels increases to the point where Porter-Thomas fluctuations are sufficiently reduced so that they become comparable to experimental errors. However, if only this energy region is used, the uncertainties of the shapes of the output strength functions become considerably larger.

Detailed calculations show that the main contribution to the TSC intensity comes from cascades with hard primary transitions whose energies exceed half of the sum of the cascade energies, i.e. $E_{\gamma 1} > (E_{\gamma 1} + E_{\gamma 2})/2$. These transitions populate the lower half of the accessible

excitation-energy region of ^{60}Ni , where levels of positive parity dominate. Taking into account that for this reaction, s-wave protons populate 3^- and 4^- spins in about 90% of the cases, the cascades populating the 2^+ final level have $E1+M1$ multipolarity with $E_{\gamma 2}^{M1} < 5 \text{ MeV}$. That is why the TSC spectrum in our experiment is sensitive to low-energy $M1$ strength. In other nuclei the situation might be different.

V. CONCLUSION

In this paper the two-step cascade method previously developed and used for neutron-capture experiments, has been applied to proton-capture reactions. The advantage of the proton TSC spectra is the possibility to get the absolute TSC intensities with much greater precision compared to TSC intensities from neutron-capture reactions. Secondly, the proton TSC spectra undergo less PT fluctuations. This fact allows us to put more restrictions on the range of possible γ -strength functions describing the experimental TSC spectra.

A simulation technique has been used to infer strength functions capable to describe the experimental spectrum.

The obtained $M1$ strength functions support strongly a low-energy increase resulting in a similar increase in the sum of the $E1+M1$ strength functions. This increase is consistent with what is observed for nuclei in the same mass region (iron nuclei from Oslo-type experiments [6, 7]). However, the TSC spectrum from the $^{59}\text{Co}(p, 2\gamma)$ reaction is not sensitive enough to determine whether there is a low-energy enhancement of the $E1$ γ -strength

function.

In conclusion, we have demonstrated in this work that the combination of analyzing TSC spectra from proton-capture reactions along with measuring level densities from particle-evaporation experiments is a good supplementary tool to study both $E1$ and $M1$ strength functions in atomic nuclei.

-
- [1] E. Litvinova, H. Loens, K. Langankea, G. Martinez-Pinedo, T. Rauscher, P. Ringf, F.-K. Thielemann, and V. Tselyaev, *Nucl. Inst. Meth.* **A823**, 26 (2009).
- [2] T. Belgia, O. Bersillon, R. Capote, T. Fukahori, G. Zhang, S. Goriely, M. Herman, A. V. Ignatyuk, S. Kailas, A. Koning, et al., *Handbook for calculations of nuclear reaction data: Reference input parameter library*, available at <http://www-nds.iaea.org/RIPL-2/> (2005).
- [3] D. Savran, M. Fritzsche, J. Hasper, K. Lindenberg, S. Muller, V.Y. Ponomarev, K. Sonnabend, and A. Zilges, *Phys. Rev. Lett.* **100**, 232501 (2008).
- [4] U. Agvaanluvsan, A.C. Larsen, R. Chankova, M. Guttormsen, G.E. Mitchell, A. Schiller, S. Siem, and A. Voinov, *Phys. Rev. Lett.* **102**, 162504 (2009).
- [5] G. Rusev, R. Schwengner, R. Beyer, M. Erhard, E. Grosse, A.R. Junghans, K. Kosev, C. Nair, K.D. Schilling, A. Wagner, et al., *Phys. Rev.* **C79**, 061302(R) (2009).
- [6] A. V. Voinov, S. M. Grimes, C. R. Brune, M. J. Hornish, T. N. Massey, and A. Salas, *Phys. Rev.* **C76**, 044602 (2007).
- [7] E. Algin, A. Schiller, A. Voinov, U. Agvaanluvsan, T. Belgia, L. Bernstein, C. R. Brune, R. Chankova, P. E. Garrett, S. M. Grimes, et al., *Phys. Atomic Nuclei* **70**, 1634 (2007).
- [8] A. Larsen, R. Chankova, M. Guttormsen, F. Ingelbretsen, S. Messelt, J. Rekstad, S. Siem, N. Syed, S. Ødegård, T. Lönnroth, et al., *Phys. Rev.* **C73**, 064301 (2006).
- [9] M. Guttormsen, R. Chankova, U. Agvaanluvsan, E. Algin, L. Bernstein, F. Ingelbretsen, T. Lönnroth, S. Messelt, G. Mitchell, J. Rekstad, et al., *Phys. Rev.* **C71**, 044307 (2005).
- [10] A. Hoogenboom, *Nucl. Inst. Meth.* **3**, 57 (1958).
- [11] S. Boneva, E. Vasileva, Y. Popov, A. Sukhovi, and V. Khitrov, *Bull. Acad. Sci. USSR, Phys. Ser.* **52**, 1 (1988).
- [12] F. Bečvář, P. Cejnar, R. E. Chrien, and J. Kopecky, *Phys. Rev.* **C46**, 1276 (1992).
- [13] F. Bečvář, J. Honzátko, M. Krčička, S. Pašić, G. Rusev, and I. Tomandl, *Nucl. Inst. Meth.* **B261**, 930 (2007).
- [14] A. Anttila, J. Keinonen, M. Hautala, and I. Forsblom, *Nucl. Inst. Meth.* **147**, 501 (1977).
- [15] A. V. Voinov, B. M. Oginni, S. M. Grimes, C. R. Brune, M. Guttormsen, A. C. Larsen, T. N. Massey, A. Schiller, and S. Siem, *Phys. Rev.* **C79**, 031301(R) (2009).
- [16] S. Hilaire and S. Goriely, *Nucl. Phys.* **A779**, 63 (2006).
- [17] S. Kadmsky, V. Markushev, and V. Furman, *Sov. J. Nucl. Phys.* **37**, 165 (1983).
- [18] J. Kopecky and M. Uhl, *Phys. Rev.* **C41**, 1941 (1990).
- [19] M. Blatt and V. Weisskopf, *Theoretical nuclear physics*, Wiley, New York (1952).
- [20] A. Koning and J. Delaroche, *Nucl. Phys.* **A713**, 231 (2003).